= 1.70 Å and r_{cov} = 1.02 Å) and selenium (r_{ion} = 1.84 Å and r_{cov} = 1.17 Å). The zinc–carbon bond length (1.92 Å) is within the limits reported for other zinc alkyls.[12,25–28]

The packing involves two independent molecules with different orientations with respect to each other within the unit cell; there are no short or unusual contacts between the molecules. We had hoped that the use of the larger neopentyl alkyl group might lead to a structure different from that observed for the earlier compounds we have studied; unfortunately, this is not found to be the case.

Spectroscopic Studies. ^{1}H NMR spectra show a quartet and triplet for the *N*-ethyl groups (1–4), singlets for the methylene and methyl protons of neopentyl (1 and 2), and a singlet for the methyl protons of the *tert*-butyl group (3 and 4). These singlets can easily be assigned to the corresponding protons by the differences in their intensities. Only a small change in chemical shift is observed from thio- to selenocarbamates, but a significant shift to lower field is noted for the methyl protons as one goes from the neopentyl to the *tert*-butyl group. A slight change is noted in the chemical shift of *N*-ethyl protons as the alkyl substituent at the metal is varied.[13,15]

Proton-decoupled ^{13}C NMR spectroscopy reveals six- and five-line spectra for neopentyl and *tert*-butyl derivatives, respectively. A considerable difference in chemical shift is observed in the ^{13}C spectra between the thio- and selenocarbamates, especially for the $-CS_2-$/$-CSe_2-$ carbons. Similar differences in chemical shift have been noted for the methyl- and ethylzinc derivatives of thio- and selenocarbamates.[13,15] The quaternary carbons appear at lower field in the neopentyl derivatives than in the *tert*-butyl derivatives as the quaternary carbon in the *tert*-butyl group is more shielded.

The infrared spectra show the expected bands for Zn–S/Zn–Se, Zn–C, C–S/C–Se, and C–N stretching. A large decrease in stretching frequency is observed from Zn–S to Zn–Se, as expected, due to the larger mass of Se.

The similarity of the spectroscopic properties of all of the compounds strongly suggests that all the solids contain similar dimeric units.

Deposition of Thin Films. Using compounds 1–4, thin specular films of zinc chalcogens were deposited onto glass at 450 °C, under continuous vacuum, as described previously.[14] Electron microscopy showed these films to be polycrystalline with ca. 1-μm crystallites. The optical band gaps measured at room temperature were 2.70 eV for ZnSe films grown from either 1 or 3 (lit.[29] 2.70 eV; and 3.72 eV for ZnS film grown from 2 and 3.70 eV for the film grown from 4 (lit.[29] 3.68 eV). The elemental composition of the films was confirmed by elemental detection analytical X-ray methods (EDAX).

Acknowledgment. We thank the SERC for a grant to P.O'B. and for their support of crystallography at QMW.

Supplementary Material Available: Tables listing fractional atomic coordinates, anisotropic temperature factors, bond distances and angles, and selected inter- and intramolecular nonbonded distances (9 pages). Ordering information is given on any current masthead page.

OM9201977

---

(25) Bell, N. A.; Moseley, P. T. *J. Organomet. Chem.* **1987**, *325*, 47.

(26) Pajerski, A. D.; BergStresser, G. L.; Parvez, M.; Richey, H. G. *J. Am. Chem. Soc.* **1988**, *110*, 4844.

(27) Gorrel, I. B.; Looney, A.; Parkin, G. *J. Chem. Soc., Chem. Commun.* **1990**, 220.

(28) Hursthouse, M. B.; Motevalli, M.; O'Brien, P.; Walsh, J. R.; Jones, A. C. *J. Mater. Chem.* **1991**, *1*, 139.

(29) *Microelectronic Materials*; Grovenor, C. R. M., Ed.; Adam Hilger: Bristol, U.K., 1989.

Base-Induced Migrations from Iron to the η^5-Indenyl Ligand in the Complexes $(\eta^5\text{-}C_9H_7)Fe(CO)_2R$ (R = Silyl, Oligosilyl)[1]

Keith Pannell,* Jorge Castillo-Ramirez, and Francisco Cervantes-Lee
Department of Chemistry, The University of Texas at El Paso, El Paso, Texas 79968-0513

Received March 26, 1992

Summary: The complexes $(\eta^5\text{-}C_9H_7)Fe(CO)_2R$ (R = $SiMe_3$, Si_2Me_5, Si_3Me_7, Si_4Me_9, c-Si_6Me_{11}) have been synthesized, and their reactivity toward *i*-Pr_2NLi (LDA) has been examined. Intermediate salts, $[(\eta^5\text{-R-}C_9H_6)Fe(CO)_2]^-Li^+$, were formed and quenched with MeI or Ph_3SnCl. The resulting complexes were shown by spectroscopy to involve migration of the R group to the 1-position of the indenyl ligand. In the case of the migrated product $(\eta^5\text{-1-SiMe}_3\text{-}C_9H_6)Fe(CO)_2SnPh_3$ a second treatment with LDA followed by addition of Ph_3SnCl or MeI produced $(\eta^5\text{-1-SiMe}_3\text{-3-SnPh}_3\text{-}C_9H_5)Fe(CO)_2R''$ (R'' = Ph_3Sn, Me). The complex with R'' = Ph_3Sn was characterized by single-crystal X-ray analysis to confirm the location of the migrated groups.

Migration of silyl, germyl, stannyl, and plumbyl groups from transition-metal centers to η^5-cyclopentadienyl ligands upon initial deprotonation of the cyclopentadienyl ligand has been studied extensively.[2] Related migrations of certain acyl and substituted alkyl groups have also been reported.[3] Given the relationship between the cyclopentadienyl and indenyl ligands, and the often greater reactivity of the indenyl system due to the η^5–η^3 ring-

---

(1) Organometalloidal Derivatives of the Transition Metals. 32. Part 31: Pannell, K. H.; Kobayashi, T.; Kapoor, R. N. *Organometallics* **1992**, *11*, 2229.

(2) (a) Dean, W. K.; Graham, W. A. G. *Inorg. Chem.* **1977**, *16*, 1060. (b) Berryhill, S. R.; Sharenow, B. J. *J. Organomet. Chem.* **1981**, *221*, 143. (c) Thum, G.; Ries, W.; Malisch, W. *J. Organomet. Chem.* **1983**, *252*, C67. (d) Berryhill, S. R.; Clevenger, G. L.; Burdurli, Y. P. *Organometallics* **1985**, *4*, 1509. (e) Heah, P. C.; Gladysz, J. A. *J. Am. Chem. Soc.* **1984**, *106*, 7636. (f) Crocco, G. L.; Gladysz, J. A. *J. Chem. Soc., Chem. Commun.* **1985**, 283. (g) Pannell, K. H.; Hernandez, C.; Cervantes, J.; Cassias, J.; Vincenti, S. P. *Organometallics* **1986**, *5*, 1056. (h) Crocco, J. L.; Young, C. S.; Lee, K. E.; Gladysz, J. A. *Organometallics* **1988**, *7*, 2158. (i) Cervantes, J.; Vincenti, S. P.; Kapoor, R. N.; Pannell, K. H. *Organometallics* **1989**, *8*, 744. (j) Berryhill, S. R.; Corriu, R. J. P. *J. Organomet. Chem.* **1989**, *370*, C1.

(3) (a) Abbott, S.; Baird, G. J.; Davies, S. G.; Dordor-Hedgecock, I. M.; Maberly, T. D.; Walker, J. C.; Warner, P. *J. Organomet. Chem.* **1985**, *289*, C17. (b) Heah, P. C.; Patton, A. T.; Gladysz, J. A. *J. Am. Chem. Soc.* **1986**, *108*, 1185. (c) Pannell, K. H.; Vincenti, S. P.; Scott, R., III. *Organometallics* **1987**, *6*, 1593. (d) Sharma, S.; Kapoor, R. N.; Cervantes-Lee, F.; Pannell, K. H. *Polyhedron* **1991**, *11*, 1177.

0276-7333/92/2311-3139$03.00/0 © 1992 American Chemical Society

Table I. Yield, Melting Point, Elemental Analysis, and Spectral Data for the Complexes[a]

$(\eta^5\text{-}C_9H_7)Fe(CO)_2R$

R = $SiMe_3$: 31%; 75–76 °C; ^{1}H NMR 0.35 (Me), 7.45, 7.18, 4.89 (C_9H_7); ^{13}C NMR 7.24 (Me), 71.7, 91.9, 105.4, 124.1, 126.5 (C_9H_7); ^{29}Si NMR 47.5; IR ν(CO) 1986. 1931. Anal. Calcd (Found): C, 56.00 (55.90); H, 5.37 (5.33).

R = $SiMe_2SiMe_3$: 50%; 59–60 °C; ^{1}H NMR 0.46, 0.22 (Me), 7.09, 6.83, 4.89 (C_9H_7); ^{13}C NMR −0.16, 3.67 (Me), 72.0, 90.9, 105.8, 124.5, 127.0 (C_9H_7); ^{29}Si NMR −11.9, 25.1; IR ν(CO) 1986, 1933. Anal. Calcd (Found): C, 53.60 (53.40); H, 6.19 (6.23).

R = $SiMe_2SiMe_2SiMe_3$: 42%; 58–59 °C; ^{1}H NMR 0.37, 0.19, 0.08 (Me), 7.48, 7.17, 4.96 (C_9H_7); ^{13}C NMR −4.43, −1.21, 4.95 (Me), 71.6, 90.4, 105.4, 124.1, 126.6 (C_9H_7); ^{29}Si NMR −36.6, −15.2, 30.0; IR ν(CO) 1986, 1932. Anal. Calcd (Found): C, 51.90 (51.55); H, 6.78 (6.92).

R = $SiMe_2(SiMe_2)_2SiMe_3$: 10%; 59–60 °C; ^{1}H NMR 0.40, 0.27, 0.14, 0.09 (Me), 7.47, 7.20, 5.00 (C_9H_7); ^{13}C NMR −5.08, −2.73, −0.71, 5.71, 72.01, 90.7, 105.8, 124.5, 127.1 (C_9H_7); ^{29}Si NMR −43.2, −32.8, −15.2, 31.0; IR ν(CO) 1987, 1933. Anal. Calcd (Found): C, 50.60 (49.22); H, 7.28 (7.08).

R = $SiMe(SiMe_3)_2$: 40%; 85–86 °C; ^{1}H NMR 0.20, 0.16 (Me), 7.47, 7.21, 4.99 (C_9H_7); ^{13}C NMR −3.01, 1.44 (Me), 71.8, 89.3, 105.4, 124.5, 127.18 (C_9H_7); ^{29}Si NMR −12.7, −8.7; IR ν(CO) 1987, 1934. Anal. Calcd (Found): C, 51.90 (51.70); H, 6.78 (6.72).

R = $Si(SiMe_3)_3$: 43%; 74–75 °C; ^{1}H NMR 0.19 (Me), 7.48, 7.21, 5.20, 5.05 (C_9H_7); ^{13}C NMR 3.84 (Me), 72.4, 89.5, 105.1, 124.7, 127.59 (C_9H_7); ^{29}Si NMR −69.5, −6.30; IR ν(CO) 1989, 1939. Anal. Calcd (Found): C, 50.60 (50.13); H, 7.23 (7.30).

R = Si_6Me_{11}: 22%; 124–125 °C; ^{1}H NMR 0.37, 0.29, 0.14 (Me), 7.48, 7.24, 5.12 (C_9H_7); ^{13}C NMR −6.05, −4.16, −1.18, 0.02 (Me), 70.1, 89.2, 105.6, 124.5, 127.22 (C_9H_7); ^{29}Si NMR −42.8, −39.9, −29.4, −3.7; IR ν(CO) 1987, 1936. Anal. Calcd (Found): C, 47.10 (47.37); H, 7.13 (7.33).

$(\eta^5\text{-}R\text{-}C_9H_6)Fe(CO)_2R'$

Ia (R = $SiMe_3$, R′ = Me): 73%; oil; ^{1}H NMR 0.29, −0.23 (Me), 4.97, 4.38, 7.11, 7.00, 6.78 (C_9H_6); ^{13}C NMR −16.2 (FeMe), 0.0 (SiMe), 77.3, 78.7, 97.7, 105.7, 111.2, 124.8, 125.7, 127.4 (C_9H_6), 217.6, 218.5 (CO); ^{29}Si NMR −3.96; IR ν(CO) 2000, 1943. Anal. Calcd (Found): C, 57.33 (56.88); H, 5.77 (5.89).

Ib (R = $SiMe_3$, R′ = $SnPh_3$: 64%; 185–186 °C; ^{1}H NMR 0.15 (Me), 4.68, 4.91, 7.77, 6.92 (C_9H_6, Ph); ^{13}C NMR −0.11 (Me), 74.5, 81.2, 91.4, 106.1, 106.7, 125.0, 126.5, 127.2, 127.7, 137.4, 144.6 (C_9H_6, Ph), 215.2, 216.1 (CO); ^{29}Si NMR −0.53; IR ν(CO) 1987, 1939. Anal. Calcd (Found): C, 59.20 (54.00); H, 4.66 (3.99).

IIa (R = $SiMe_2SiMe_3$, R′ = Me): 75%; oil; ^{1}H NMR −0.19, 0.01, 0.40, 0.59 (Me), 4.12, 5.00, 7.17, 7.00, 6.83 (C_9H_6); ^{13}C NMR −16.3 (FeMe), −3.54, −2.38, −2.08 (SiMe), 77.2, 78.8, 96.9, 106.0, 110.7, 125.0, 125.3, 126.5, 127.0 (C_9H_6), 217.7, 218.3 (CO); ^{29}Si NMR −22.2, −19.2; IR ν(CO) 2000, 1943. Anal. Calcd (Found): C, 53.82 (53.78); H, 6.50 (6.94).

IIb (R = $SiMe_2SiMe_3$, R′ = $SnPh_3$): 62%; 180–181 °C; ^{1}H NMR −0.10, 0.05, 0.54 (Me), 5.24, 7.63, 7.16, 7.08 (C_9H_6, Ph); ^{13}C NMR −4.50, −2.74, −2.09 (Me), 81.4, 86.2, 98.1, 109.6, 110.7, 126.0, 126.3, 137.6, 144.1 (C_9H_6, Ph), 215.2, 216.9 (CO); ^{29}Si NMR −21.4, −18.1; IR ν(CO) 1986, 1938. Anal. Calcd (Found): C, 57.73 (57.47); H, 5.13 (4.98).

IIIa (R = $SiMe_2SiMe_2SiMe_3$, R′ = Me): 44%; oil; ^{1}H NMR −0.25, −0.04, −0.01, 0.65 (Me), 4.12, 4.99, 7.15, 6.95, 6.79 (C_9H_6); ^{13}C NMR −16.2 (FeMe), −6.36, −2.45, −1.49 (SiMe), 77.0, 79.5, 96.8, 106.3, 110.3, 124.0, 126.6, 126.9 (C_9H_6), 217.7, 218.2 (CO); ^{29}Si NMR −47.1, −18.7, −15.8; IR ν(CO) 1998, 1942. Anal. Calcd (Found): C, 53.00 (53.73); H, 7.02 (7.62).

IVb (R = $SiMe(SiMe_3)_2$, R′ = $SnPh_3$): 51%; 97–98 °C; ^{1}H NMR 0.12, 0.18, 0.54 (Me), 4.43, 5.02, 7.73, 7.20 (C_9H_6, Ph); ^{13}C NMR −7.70, −0.72, −0.42 (Me), 75.8, 81.6, 89.2, 104.3, 105.7, 125.3, 126.1, 137.7, 144.1 (C_9H_6, Ph), 215.3, 217.0 (CO); ^{29}Si NMR −47.9, −14.9; IR ν(CO) 1985, 1938. Anal. Calcd (Found): C, 56.48 (56.11); H, 5.53 (5.63).

Va (R = $(SiMe_2)_3SiMe_3$, R′ = Me): 30%; oil; ^{1}H NMR −0.21, 0.05, 0.45, 0.70 (Me), 4.46, 5.01, 7.19, 6.98, 6.81 (C_6H_7); ^{13}C NMR −16.1 (FeMe), −5.75, −5.40, −5.02, −2.18, −1.12 (SiMe), 77.1, 96.6, 106.3, 110.4, 125.3, 126.7, 126.9 (C_9H_6), 217.7, 218.3 (CO); ^{29}Si NMR −15.7, −17.8, −43.4, −44.3; IR ν(CO) 1999, 1942.

VIa (R = $Si(SiMe_3)_3$, R′ = Me): 65%; 86–87 °C; ^{1}H NMR −0.27, 0.27 (Me), 4.68, 4.90, 6.82, 7.34 (C_9H_6); ^{13}C NMR −14.9 (FeMe), 2.05 (SiMe), 77.0, 96.1, 96.8, 107.2, 109.7, 124.8, 126.1, 126.6, 126.9 (C_9H_6), 218.0, 218.2 (CO); ^{29}Si NMR −83.5, −12.3; IR ν(CO) 1998, 1942. Anal. Calcd (Found): C, 51.61 (51.38); H, 7.42 (7.43).

VIIa (R = Si_6Me_{11}, R′ = Me): 55%; oil; ^{1}H NMR −0.16, 0.26, 0.82 (Me), 4.70, 4.97, 6.87, 7.20, 7.36 (C_9H_6); ^{13}C NMR −16.2 (FeMe), −6.63, −5.91, −5.31, −3.97, −3.50 (SiMe), 76.3, 79.0, 96.5, 108.5, 108.6, 124.5, 126.3, 126.4, 127.1 (C_9H_6), 217.8, 218.2 (CO); ^{29}Si NMR −42.1, −42.0, −41.3, −41.2, −40.2, −39.7; IR ν(CO) 1998, 1941. Anal. Calcd (Found): C, 49.05 (49.17); H, 7.36 (7.37).

$(\eta^5\text{-}R\text{-}R'\text{-}C_9H_5)Fe(CO)_2R''$

VIIIa (R = $SiMe_3$, R′ = $SnPh_3$, R″ = Me): 54%; 97–98 °C; ^{1}H NMR −0.13, 0.30 (Me), 5.00, 7.16, 7.81 (C_9H_5, Ph); ^{13}C NMR −16.4 (FeMe), 0.0 (SiMe), 77.7, 83.4, 105.4, 112.8, 113.2, 125.7, 126.5, 127.1, 127.2, 129.2, 129.8, 136.6, 136.7 (C_9H_5, Ph), 217.6, 217.8 (CO); ^{29}Si NMR −3.51; IR ν(CO) 1998, 1943. Anal. Calcd (Found): C, 59.67 (59.22); H, 5.00 (4.89).

VIIIb (R = $SiMe_3$, R′ = $SnPh_3$, R″ = $SnPh_3$): 43%; 192–193 °C; ^{1}H NMR 0.37 (Me), 5.64, 7.37, 7.83 (C_9H_5, Ph); ^{13}C NMR −0.40 (Me), 80.3, 84.8, 99.4, 109.7, 110.5, 126.1, 126.6, 129.0, 129.5, 137.1, 137.4, 138.4, 144.0 (C_9H_5, Ph), 215.9 (CO); ^{29}Si NMR −2.86; IR ν(CO) 1988, 1939. Anal. Calcd (Found): C, 60.2 (60.0); H, 4.44 (4.60).

[a] IR data (cm^{-1}) were recorded in THF; ^{13}C, ^{29}Si, and ^{1}H NMR spectra (δ) were recorded in C_6D_6 ($(\eta^5\text{-}C_9H_7)Fe(CO)_2R$) or $CDCl_3$ (migrated products).

slippage process,[4] we have investigated the reactivity of the complexes $(\eta^5\text{-}C_9H_7)Fe(CO)_2R$ (R = silyl, oligosilyl) toward treatment with the base lithium diisopropylamide (LDA).

Experimental Section

NMR data were recorded using a Bruker AC/200 FT NMR spectrometer, infrared spectra on a Perkin-Elmer 1600 FTIR spectrophotometer using 0.1 mm path length NaCl cells, and UV/visible data on a Perkin-Elmer Lambda 4L UV/vis spectrophotometer. A Varian Aerograph Series 1400 gas chromatograph with a thermal conductivity bridge detector equipped with a 6 ft × $^1/_8$ in. stainless steel column, packed with 10% OV 101 on Chromosorb W-HP 100/120 (Alltech Associates Inc.), was used to determine purity in each step of the synthesis of the chlorosilanes. Elemental analyses were performed by Galbraith Laboratories Inc.

The following chemicals were obtained from the sources indicated: alumina (80–200 mesh), from Fisher Scientific Co.; silica gel (60/200 mesh), from Mallinkrodt Inc.; $Fe(CO)_5$, *n*-butyllithium, diisopropylamine, indene, sodium, lithium, $AlCl_3$, methyl iodide, HCl(g), and $SbCl_5$, from Aldrich Chemical Co.; Ph_3SnCl, from Alfa; Me_3SiCl, $PhMe_2SiCl$, Me_6Si_2, and $HSiCl_3$, from Petrarch Systems Inc. All reactions were performed under an atmosphere of N_2 in oven-dried glassware using dry and oxygen-free solvents. Starting organosilicon and metal compounds were synthesized by literature procedures: $Me_3Si(SiMe_2)_nCl$ (n = 1,[5] 2,[6] 3[7]);

---

[4] Lobanova, I. A.; Zdanovich, V. I. *Russ. Chem. Rev. (Engl. Transl.)* **1988**, *57*, 967.

[5] Sakurai, H.; Tominaga, K.; Watanabe, T.; Kumada, M. *Tetrahedron Lett.* **1966**, 5493.

[6] Kumada, M.; Ishikawa, M.; Maeda, S. *J. Organomet. Chem.* **1964**, *2*, 478.

[7] Boberski, W. G.; Allred, A. L. *J. Am. Chem. Soc.* **1974**, *96*, 1244.

$\mathrm{(Me_3Si)_2MeSiCl}$;[6] $\mathrm{(Me_3Si)_3SiCl}$;[8] $\mathrm{Me_{11}Si_6Cl}$;[9] $\mathrm{[(\eta^5\text{-}C_9H_7)Fe(CO)_2]_2}$.[10]

Synthesis of $\mathbf{(\eta^5\text{-}C_9H_7)Fe(CO)_2R}$ Complexes. A sodium/mercury amalgam was made by dissolving 0.26 g (11.3 mmol) of Na in 40 g of Hg in a 250-mL side-arm flask equipped with a magnetic stirring bar and a rubber septum. To this amalgam was added 2.57 g (5.65 mmol) of $\mathrm{[(\eta^5\text{-}C_9H_7)Fe(CO)_2]_2}$ and 60 mL of THF. After the mixture was vigorously shaken for 30 min, the color of the solution changed to orange, indicating the formation of the anion $\mathrm{[(\eta^5\text{-}C_9H_7)Fe(CO)_2]^-Na^+}$ (IR monitoring of the anion showed ν(CO) bands at 1882, 1867, 1815, and 1780 $\mathrm{cm^{-1}}$ in THF). The excess amalgam was drained out through the side arm, and a solution of 11 mmol of the appropriate chlorosilane in 20 mL of THF was added dropwise to the reaction mixture at 0 °C. The mixture was warmed to room temperature and stirred for 3 h, after which time IR monitoring showed two ν(CO) bands characteristic of $\mathrm{(\eta^5\text{-}L)Fe(CO)_2R}$ complexes. The solvent was removed under vacuum and the residue dissolved in 60 mL of a 2% (v/v) THF in hexane solvent mixture. The solution was filtered through 4 cm of alumina using a Buchner funnel, and the volume was reduced to 5 mL under vacuum. This concentrated solution was placed upon a 2.0 × 35 cm silica gel column and elution with hexane developed a yellow band which was collected. After removal of the solvent a yellow solid was obtained which was purified by sublimation to remove the traces of indene and other small impurities. The temperatures used for removing impurities from the complexes $\mathrm{(\eta^5\text{-}C_9H_7)Fe(CO)_2R}$ were as follows (°C/0.1 mmHg): 46–48, R = $\mathrm{SiMe_3}$, $\mathrm{SiMe_2SiMe_3}$; 48–53, R = $\mathrm{SiMe_2SiMe_2SiMe_3}$, $\mathrm{SiMe(SiMe_3)_2}$; 68–70, R = $\mathrm{SiMe_2(SiMe_2)_2SiMe_3}$; 88–90, R = $\mathrm{Si(SiMe_3)_3}$; 110, R = $\mathrm{Si_6Me_{11}}$ (cyclic). The sublimation temperatures used were as follows (°C/0.1 mmHg): 58–60, R = $\mathrm{SiMe_3}$, $\mathrm{Si_2Me_5}$; 60–62, R = $\mathrm{Si_3Me_7}$, $\mathrm{SiMe(SiMe_3)_2}$; 108–110, R = $\mathrm{Si(SiMe_3)_3}$; 80–82, R = $\mathrm{(SiMe_2)_3SiMe_3}$. The analytical data, yields, and spectroscopic data are reported in Table I.

Synthesis of $\mathbf{(\eta^5\text{-}1\text{-}R\text{-}C_9H_6)Fe(CO)_2R'}$ Complexes. Preparation of Lithium Diisopropylamide (LDA). In a 50-mL side-arm flask equipped with a magnetic stirring bar and a rubber septum was placed 10 mL of THF and 1 mL (7.1 mmol) of diisopropylamine. The resulting solution was stirred at 0 °C for 15 min, after which 4.3 mL (6.9 mmol) of *n*-butyllithium (1.6 M in hexane) was added and the mixture stirred for 15 min at 0 °C. This provided 15.3 mL of an LDA solution (4.5×10^{-1} M).

Preparation of $\mathbf{(\eta^5\text{-}1\text{-}R\text{-}C_9H_6)Fe(CO)_2R'}$ Complexes. In a typical reaction, 3.3 mmol of $\mathrm{(\eta^5\text{-}C_9H_7)Fe(CO)_2R}$ in 80 mL of THF was placed in a side-arm flask equipped with a magnetic stirring bar and a rubber septum. To this solution was slowly added 1.3 equiv of freshly prepared LDA at 0 °C. The initially yellow solution immediately became dark orange-brown and the solution was stirred for 10–20 min at 0 °C. The IR spectrum indicated that all of the starting material had been consumed and replaced by a new complex with three ν(CO) bands at 1868, 1797, and 1755 $\mathrm{cm^{-1}}$. To this solution was added an excess of methyl iodide (or 1 equiv in the case of $\mathrm{Ph_3SnCl}$ in 20 mL of THF), and the solution immediately changed color to yellow-brown. The IR spectrum of this solution showed two ν(CO) bands in the region expected for $\mathrm{(\eta^5\text{-}C_9H_5R)Fe(CO)_2R'}$. This solution was stirred for 30 min, and then the solvent was removed under vacuum. The residue was dissolved in the minimum amount of a hexane/THF (98:2) solvent mixture and the solution placed upon a 2 × 35 cm silica gel column. Elution with hexane developed a yellow band which was collected. Evaporation of the solvent yielded the migrated product $\mathrm{(\eta^5\text{-}1\text{-}R\text{-}C_9H_6)Fe(CO)_2R'}$. Elemental analyses, yields, and spectral data are presented in Table I.

Synthesis of $\mathbf{(\eta^5\text{-}1\text{-}SiMe_3\text{-}3\text{-}SnPh_3\text{-}C_9H_5)Fe(CO)_2R''}$ Complexes. The procedure for the synthesis of $\mathrm{(\eta^5\text{-}1\text{-}R\text{-}C_9H_6)Fe(CO)_2R'}$ (R = $\mathrm{SiMe_3}$, R′ = $\mathrm{SnPh_3}$) was the same as described above. After addition of the solution of $\mathrm{ClSnPh_3}$ to the anion, the mixture was stirred for 20 min and 1.3 equiv of LDA then was added. The solution changed color to red-brown and the IR spectrum showed the presence of the anion (ν(CO) 1867, 1797, and 1755 $\mathrm{cm^{-1}}$). After it was stirred for 15 min at 0 °C the solution was quenched with MeI (or 1 equiv of $\mathrm{ClSnPh_3}$) and stirred for 15 min. The IR spectrum of this solution showed the presence of the same pattern of peaks in the carbonyl region as for the related starting material. The solvent was then removed under vacuum, the residue was dissolved in the minimum amount of a hexane/THF mixture (98:2), and this solution was placed upon a 2 × 35 cm silica gel column. Elution with a hexane/THF (98:2) solvent mixture developed a yellow band, which was collected. From this solution was isolated the double-migrated product $\mathrm{(\eta^5\text{-}1\text{-}SiMe_3\text{-}3\text{-}SnPh_3\text{-}C_9H_5)Fe(CO)_2R''}$. The elemental analyses, yields, and spectral data are recorded in Table I.

Structural Determination of $\mathbf{(\eta^5\text{-}Me_3Si\text{-}Ph_3Sn\text{-}C_9H_5)Fe(CO)_2SnPh_3}$. X-ray data were collected on a Nicolet R3m/V four-circle diffractometer at room temperature, using graphite-monochromated Mo Kα radiation (λ = 0.71073 Å) and the ω-scan mode with variable speed between 3.0 and 15.0° $\mathrm{min^{-1}}$ and a scan range of 1.2°. Three check reflections were monitored every 1 h, and their intensities remained constant, showing no evidence of crystal decay during the experiment. The structure was solved by direct methods and refined by anisotropic full-matrix least squares minimizing $\sum w(F_o - F_c)^2$. Structure solution and refinement were carried out with the SHELXTL-PLUS crystallographic software on a Microvax II computer. Hydrogen atoms were located at idealized positions from assumed geometries and included in least-squares and structure factor calculations as riding atoms with isotropic thermal parameters fixed at 0.08 $\mathrm{Å^2}$. A semiempirical absorption correction was applied, giving a minimum/maximum transmission ratio of 0.24/0.26. Relevant crystal data and parameters used for data collection and structure refinement are summarized in Table II; atomic coordinates are presented in Table III, and selected bond lengths and angles are reported in Table IV.

Results and Discussion

Treatment of the complexes $\mathrm{(\eta^5\text{-}C_9H_7)Fe(CO)_2R}$ with LDA readily produced the rearranged salt $\mathrm{[(\eta^5\text{-}R\text{-}C_9H_6)Fe(CO)_2]^-Li^+}$, which was quenched with MeI or $\mathrm{Ph_3SnCl}$ (R′X) to yield the corresponding complex $\mathrm{(\eta^5\text{-}R\text{-}C_9H_6)Fe(CO)_2R'}$ (eq 1).

$$\mathrm{(\eta^5\text{-}C_9H_7)Fe(CO)_2R} \xrightarrow{\mathrm{LDA}} \mathrm{[(\eta^5\text{-}R\text{-}C_9H_6)Fe(CO)_2]^-Li^+} \xrightarrow{\mathrm{R'X}} \underset{\mathrm{I\text{–}VII}}{\mathrm{(\eta^5\text{-}R\text{-}C_9H_6)Fe(CO)_2R'}} \qquad (1)$$

$$\mathrm{R = SiMe_3\ (I),\ SiMe_2SiMe_3\ (II),\ (SiMe_2)_2SiMe_3\ (III),\ SiMe(SiMe_3)_2\ (IV),\ (SiMe_2)_3SiMe_3\ (V),\ Si(SiMe_3)_3\ (VI),\ c\text{-}Si_6Me_{11}\ (VII)}$$

$$\mathrm{a,\ R' = Me;\ b,\ R' = Ph_3Sn}$$

In the case of product Ib a second treatment with LDA followed by addition of MeI or $\mathrm{Ph_3SnCl}$ led to the formation of a double-migration product (eq 2).

$$\mathrm{(\eta^5\text{-}Me_3Si\text{-}C_9H_6)Fe(CO)_2SnPh_3} \xrightarrow[\mathrm{(2)\ R'X}]{\mathrm{(1)\ LDA}} \underset{\mathrm{VIIIa,b}}{\mathrm{(\eta^5\text{-}Me_3Si\text{-}Ph_3Sn\text{-}C_9H_5)Fe(CO)_2R''}} \qquad (2)$$

$$\mathrm{R'' = Me\ (VIIIa),\ Ph_3Sn\ (VIIIb)}$$

We have obtained a single-crystal X-ray structure of the new complex VIIIb, and this is illustrated in Figure 1. The overall structure is unremarkable (selected bond distances and angles are recorded in Table IV), but the structure shows that the two migrations occurred to the 1- and 3-positions of the indenyl ligand. In general, the formation of indenyl derivatives from indenyllithium produces 1-substituted complexes. However, a notable exception to this is a report by Lobanova et al. on the lithiation of $\mathrm{(\eta^5\text{-}C_9H_7)Mn(CO)_3}$ followed by quenching with $\mathrm{CO_2}$ or $\mathrm{Me_3SiCl}$, in which cases both 1- and 2-substituted indenyl derivatives were reported.[11]

---

[8] (a) Bürger, H.; Killian, W. *J. Organomet. Chem.* **1969**, *18*, 299. (b) Gilman, H.; Harrell, R. L. *J. Organomet. Chem.* **1966**, *5*, 199.

[9] Mitter, F. K.; Hengge, E. *J. Organomet. Chem.* **1987**, *332*, 47.

[10] Forschner, T. C.; Cutler, A. R. *Inorg. Chim. Acta* **1985**, *102*, 113.

Table II. Structure Determination Summary for Complex VIIIb

Crystal Data	
empirical formula	$C_{50}H_{44}FeO_2SiSn_2$
color; habit	orange prism
cryst size, mm	0.32 × 0.36 × 0.40
cryst syst	orthorhombic
space group	*Pbca*
unit cell dimens	
a, Å	12.340 (4)
b, Å	18.120 (4)
c, Å	40.170 (8)
V, Å^3	8982 (4)
Z	8
fw	998.2
density (calcd), Mg/m^3	1.476
abs coeff, mm^{-1}	1.489
$F(000)$	4000
Data Collection	
diffractometer used	Siemens R3m/V
radiation	Mo Kα (λ = 0.71073 Å)
temp, K	298
monochromator	highly oriented graphite cryst
2θ range, deg	3.5–45.0
scan type	ω
scan speed, deg/min	variable; 3.00–20.00 in ω
scan range (ω), deg	1.20
bkgd measmt	stationary cryst and stationary counter at beginning and end of scan, each for 25.0% of total scan time
std rflns	3 measd every 100 rflns
index ranges	$0 \le h \le 13$, $0 \le k \le 19$, $0 \le l \le 43$
no. of rflns collected	6593
no. of indep rflns	5916 (R_{int} = 0.00%)
no. of obsd rflns	3555 ($F > 3.0\sigma(F)$)
abs cor	semiempirical
min/max transmissn	0.2378/0.2630
Solution and Refinement	
syst used	Siemens SHELXTL PLUS (VMS)
soln	direct methods
refinement method	full-matrix least squares
quantity minimized	$\sum w(F_o - F_c)^2$
absolute structure	not applicable
extinctn cor	χ = 0.000010 (6), where $F^* = F[1 + 0.002\chi F^2/(\sin 2\theta)]^{-1/4}$
H atoms	riding model, fixed isotropic U
weighting scheme	$w^{-1} = \sigma^2(F) + 0.0005F^2$
no. of params refined	506
final R indices (obsd data)	R = 5.19%, R_w = 5.29%
R indices (all data)	R = 10.31%, R_w = 6.92%
goodness of fit	1.37
largest and mean Δ/σ	0.519, 0.092
data-to-param ratio	7.0:1
largest diff peak, e/Å^3	0.73
largest diff hole, e/Å^3	−0.84

Table III. Atomic Coordinates ($\times 10^4$) and Equivalent Isotropic Displacement Coefficients (Å^2 × 10^3) for Complex VIIIb

	x	y	z	U(eq)[a]
Sn1	1765 (1)	1901 (1)	690 (1)	41 (1)
Sn2	1252 (1)	2490 (1)	1864 (1)	47 (1)
Fe	3222 (1)	1750 (1)	1148 (1)	41 (1)
Si	4832 (3)	3391 (2)	907 (1)	53 (1)
O1	4713 (8)	1111 (5)	669 (2)	73 (4)
O2	2348 (8)	297 (5)	1308 (3)	78 (4)
C1	2939 (9)	2844 (6)	1299 (3)	45 (4)
C2	2679 (9)	2357 (6)	1563 (2)	43 (4)
C3	3696 (9)	2005 (6)	1661 (3)	42 (4)
C4	3952 (11)	1514 (7)	1920 (3)	61 (5)
C5	4979 (14)	1267 (8)	1940 (3)	77 (6)
C6	5804 (12)	1501 (8)	1732 (4)	70 (6)
C7	5582 (10)	1949 (7)	1473 (3)	62 (5)
C8	4507 (9)	2230 (6)	1438 (3)	42 (4)
C9	4060 (10)	2763 (6)	1201 (3)	47 (4)
C10	1462 (9)	3016 (7)	515 (3)	44 (4)
C11	1622 (11)	3186 (7)	178 (3)	62 (5)
C12	1428 (12)	3898 (7)	59 (3)	68 (6)
C13	1069 (9)	4441 (7)	268 (3)	52 (5)
C14	899 (10)	4279 (7)	599 (3)	55 (5)
C15	1052 (9)	3577 (7)	717 (3)	49 (4)
C16	2118 (9)	1291 (7)	245 (3)	45 (4)
C17	2993 (10)	1480 (7)	35 (3)	59 (5)
C18	3178 (12)	1107 (9)	−259 (3)	68 (6)
C19	2518 (15)	545 (9)	−356 (3)	74 (6)
C20	1668 (13)	338 (8)	−163 (3)	69 (6)
C21	1464 (9)	715 (7)	137 (3)	54 (5)
C22	137 (9)	1554 (7)	825 (3)	45 (4)
C23	−701 (11)	1803 (8)	621 (3)	65 (5)
C24	−1774 (13)	1614 (10)	688 (4)	88 (7)
C25	−2022 (12)	1207 (9)	957 (5)	78 (7)
C26	−1232 (13)	957 (7)	1162 (4)	69 (6)
C27	−133 (11)	1129 (7)	1095 (3)	56 (5)
C28	197 (10)	3256 (7)	1615 (3)	49 (4)
C29	−657 (10)	3027 (8)	1418 (3)	56 (5)
C30	−1281 (12)	3535 (10)	1254 (3)	73 (6)
C31	−1089 (13)	4272 (9)	1281 (3)	72 (6)
C32	−254 (14)	4523 (7)	1463 (4)	72 (6)
C33	417 (12)	4012 (8)	1639 (3)	67 (6)
C34	335 (12)	1538 (7)	2007 (3)	53 (5)
C35	735 (16)	832 (9)	2002 (4)	89 (7)
C36	124 (23)	239 (12)	2094 (4)	125 (11)
C37	−899 (25)	332 (13)	2191 (5)	135 (13)
C38	−1339 (16)	1028 (13)	2196 (3)	100 (8)
C39	−729 (12)	1637 (9)	2101 (3)	70 (6)
C40	1863 (12)	2985 (7)	2311 (3)	58 (5)
C41	1303 (14)	2958 (8)	2603 (3)	76 (6)
C42	1715 (19)	3282 (10)	2893 (4)	105 (9)
C43	2642 (19)	3651 (10)	2882 (5)	102 (9)
C44	3205 (14)	3682 (11)	2593 (4)	100 (8)
C45	2841 (15)	3373 (10)	2311 (4)	98 (8)
C46	5710 (12)	3953 (8)	1185 (3)	84 (6)
C47	5665 (14)	2872 (8)	608 (4)	105 (7)
C48	3913 (11)	4048 (9)	699 (4)	101 (7)
C49	4093 (10)	1381 (7)	841 (3)	47 (4)
C50	2661 (10)	880 (8)	1239 (3)	52 (5)

[a] Equivalent isotropic U defined as one-third of the trace of the orthogonalized U_{ij} tensor.

Table IV. Selected Bond Lengths (Å) and Angles (deg) for Complex VIIIb

Sn1–Fe	2.585 (2)	Sn1–C16	2.147 (11)
Sn1–C22	2.174 (11)	Sn1–C10	2.171 (12)
Fe–C50	1.760 (14)	Fe–C49	1.765 (12)
C50–O2	1.158 (16)	C49–O1	1.140 (15)
Si–C48	1.845 (16)	Si–C46	1.860 (15)
Si–C9	1.895 (12)	Sn2–C2	2.148 (11)
C50–Fe–C49	92.7 (6)	Sn1–Fe–C49	88.2 (4)
Sn1–Fe–C50	88.3 (4)	Fe–C50–O2	176.0 (12)
Fe–C49–O1	173.0 (11)	C10–Sn1–C22	101.0 (4)
C10–Sn1–C16	104.1 (4)	C16–Sn1–C22	104.2 (4)
C10–Sn1–Fe	116.7 (3)	C16–Sn1–Fe	113.3 (3)
C40–Sn2–C2	103.2 (5)	C2–Sn2–C34	119.6 (5)

The spectroscopic data for the new complexes are listed in Table I. The ^{13}C NMR data for the complexes Ia,b–VIIIa,b usually exhibit nine individual resonances for the indenyl portion of the spectra, between 70 and 130 ppm in accord with migration to the 1-position of the ring. Occasionally we were unable to observe a signal for the ipso carbon atom of the ring. If the 2-position was occupied by the migrated group, then by symmetry only five resonances would have been observed. A further interesting feature of the ^{13}C spectra is the appearance of two resonances for the nonequivalent CO groups and resonances for each of the two methyl groups attached to the α-silicon in the di, tri-, and tetrasilyl groups. Both of these phenomena are expected on the basis of the location of the migrated group at the 1-position. A view of the structure

---

(11) Lobanova, I. A.; Zdanovich, V. I.; Petrovskii, P. V.; Kolobova, N. E. *J. Organomet. Chem.* **1985**, *292*, 395.

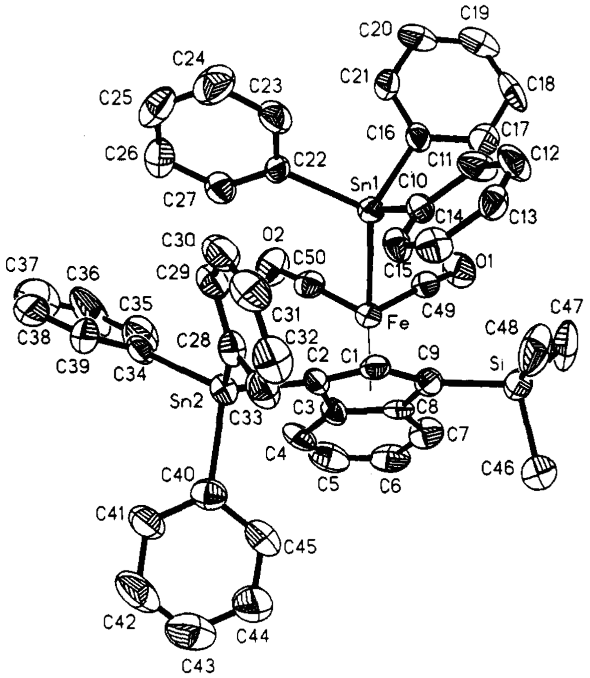

Figure 1. Structure of $(\eta^5\text{-}1\text{-}Me_3Si\text{-}3\text{-}Ph_3SnC_9H_5)Fe(CO)_2SnPh_3$ (VIIIb).

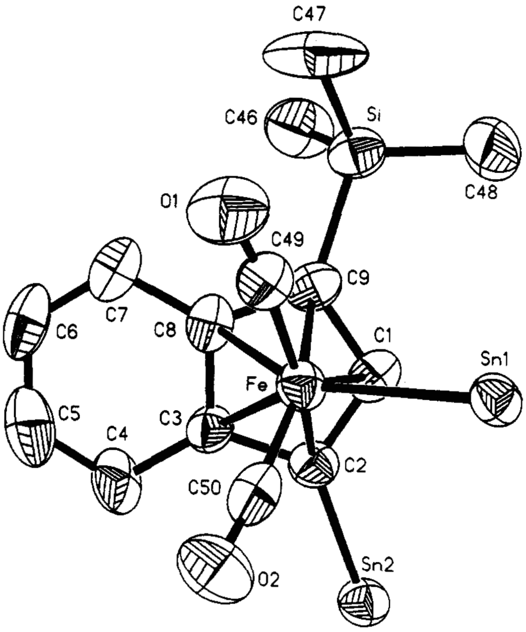

Figure 2. Structure of VIIIb viewed along the Fe–η^5-centroid axis.

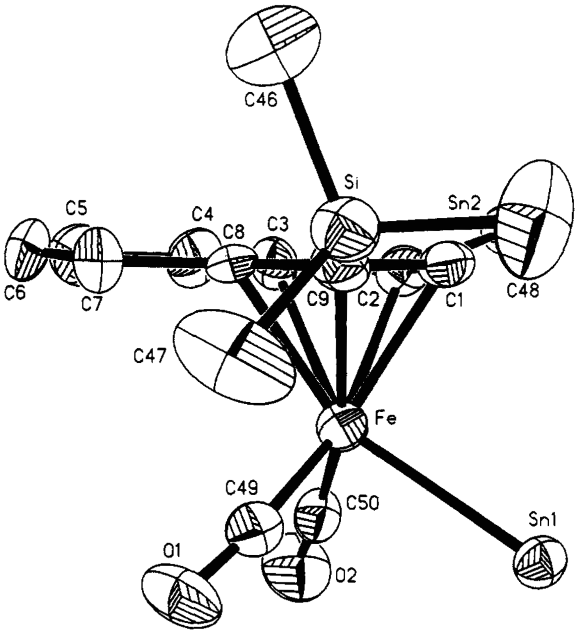

Figure 3. Structure of VIIIb viewed along the Si–C$_{indenyl}$ axis.

of VIIIb down the Fe–indenyl centroid axis (Figure 2) reveals that the two CO groups, C49–O1 and C50–O2, are in distinct chemical and magnetic environments and thus will always be nonequivalent. Similarly a view along the Si–C$_{indenyl}$ bond (Figure 3) illustrates the source of the nonequivalence of the methyl groups in II–IV, as well as the silyl groups in IV and VII (vide infra). Free rotation about the Si–C bond will not result in the equivalence of the two α-substituents on silicon in systems of the type η^5-1-Me_2RSi-C_9H_6 or η^5-1-MeR_2-C_9H_6, (R = silyl). Thus, the ^{29}Si NMR data also exhibit individual resonances for those Si atoms normally expected to be equivalent, i.e. SiMe(*Si*Me$_3$)$_2$ and SiMe(*Si*Me$_2$*Si*Me$_2$)$_2$SiMe$_2$. It is of interest that for complexes VIIIa,b the two nonequivalent CO groups are not distinguished in the ^{13}C NMR spectra, presumably due to the double substitution on the five-membered ring leveling the different chemical and magnetic environments.

Throughout our study we have been unable to detect any evidence for the migration of the silyl group to the 2-position of the indenyl five-membered ring or to the six-membered ring.

Acknowledgment. This research has been supported by the R. A. Welch Foundation, Houston, TX, the NSF (Grant No. RII-880-2973), and the DOD, Defense Logistics Agency, Directorate of Stockpile Management (Grant No. DN-009).

Supplementary Material Available: Tables of complete bond lengths and bond angles, anisotropic thermal parameters for non-hydrogen atoms, and positional and isotropic thermal parameters for hydrogen atoms (5 pages). Ordering information is given on any current masthead page.

OM9201730